J Bionic Eng 16 (2019) 1092–1102
DOI: https://doi.org/10.1007/s42235-019-0121-5

Journal of Bionic Engineering
http://www.springer.com/journal/42235

Preclinical Strength Checking for Artificial Pelvic Prosthesis under Multi-activities – A Case Study

Enchun Dong[1], Taimoor Iqbal[1], Jun Fu[2], Dichen Li[1], Bin Liu[3], Zheng Guo[2], Alberto Cuadrado[4], Zhen Zhen[3], Ling Wang[1*], Hongbin Fan[2*]

1. *State Key Laboratory for Manufacturing System Engineering*, *Xi'an Jiaotong University*, *Xi'an* 710054, *China*
2. *Department of Orthopedics*, *Xijing Hospital*, *Air Force Medical University*, *Xi'an* 710032, *China*
3. *Center for Medical Device Evaluation*, *National Medical Product Administration*, *Beijing* 100081, *China*
4. *Department of Mechanical Engineering*, *University of Las Palmas de Gran Canaria*, *Las Palmas de Gran Canaria* 35017, *Spain*

Abstract

Customized prostheses are normally employed to reconstruct the biomechanics of the pelvis after resection due to tumors or accidents. The objective of this study is to evaluate the biomechanics of the pelvis under different daily activities and to establish a functional evaluation methodology for the customized prostheses. For this purposes, finite element model of a healthy pelvis as well as a reconstructed pelvic model after type II+III resection were built for biomechanical study. The biomechanical performance of the healthy and reconstructed pelvic model was studied under routine activities including standing, knee bending, sitting down, standing up, walking, stair descent and stair ascent. Subsequently, the strength and stability of the prosthesis were evaluated under these activities. Results showed that, for the heathy pelvic model, the stresses were mainly concentrated around the upper part of the sacrum and the sacroiliac joint undergoing different activities, and the maximum stress occurred during stair ascent. As for the reconstructed pelvis, the stress distribution and the tendency of the maximum stress variation predicted for the bone part during all the activities were similar to those of the natural pelvic model, which indicated that the load transferring function of the reconstructed pelvis could be restored by the prosthesis. Moreover, the predicted maximum von Mises stress of the screws and prosthesis was below the fatigue strength of the 3D printed Ti-6Al-4V, which indicated the prosthesis can provide a reliable mechanical performance after implantation.

Keywords: pelvis, bionic prosthesis, finite element analysis, multi-activities

1 Introduction

Pelvis is one of the most important load-bearing structures in human body[1,2], and defects could happen to the pelvis due to tumors or accidents[3,4]. However, because of the complex anatomical structure and proximity of major neurovascular[5,6], it is difficult to reconstruct the pelvis after large resection[4,5,7].

Different types of pelvic prostheses have been designed and used for pelvic reconstruction[8–10]. Among those designs, the saddle prosthesis can be easily implanted during surgery[11] but fail to reconstruct the pelvic ring structure, therefore it was lessly recommended due to the associated failure rates[12,13]. Modular prothesis can restore the biomechanics of the pelvis well[14,15], however, complicated prosthetic components could increase the instability of the system and the risk of failure[16]. Customized prosthesis, with better match in terms of the geometry and fixation[3,17], becomes a suitable option for pelvic reconstruction with satisfied clinical outcomes[18].

Biomechanical analysis of the pelvis is the foundation of design and evaluation of the customized prostheses. However, the biomechanics of the pelvis is not well understood yet[19,20]. Hao *et al*.[21] studied the biomechanical performance of the pelvis under the standing stance gait by using the cadaveric pelvis. However, due to the individual characteristics of the anatomical structures and material properties of the pelvis, it is extremely hard to evaluate the customized prosthesis for each patient.

Finite Element (FE) analysis, which can accommodate large individualized differences in bone geometry and material properties[22,23], has been widely used for stud-

***Corresponding author:** Ling Wang, Hongbin Fan
E-mail: menlwang@xjtu.edu.cn, fanhb@fmmu.edu.cn

ying the biomechanics in orthopaedics. Iqbal *et al*.[8] studied the biomechanics of the healthy and customized prosthesis Reconstructed Pelvis (RP) undergoing standing phase. Volinski *et al*.[24] studied the healthy pelvic ring stresses under walking gait. Liu *et al*.[3,14] evaluated the biomechanical performance of the pelvis with an adjustable hemipelvic prosthesis under walking, stair ascent and stair descent. Even though many studies have been carried out on the biomechanics of pelvis by using FE methods, the biomechanical performance of the pelvis under all the routine activities remains unclear[3].

In this study, a customized prosthesis was designed for the pelvic reconstruction based on the clinical demands of a patient with type II+III pelvic dissection. For the functional evaluation of the designed prosthesis, FE model of both the Normal Pelvis (NP) and RP were built, and the biomechanics of the RP were studied under multi-activity loading conditions, including standing, knee bending, sitting down, standing up, walking, stair descent and stair ascent. Based on the constructed models, the strength and stability of the customized prosthesis were evaluated before the clinical application.

2 Materials and methods

2.1 Clinical information

A 43-year-old female patient, with a height of 160 cm and weight of 51 kg, was referred to Xijing Hospital (the First Affiliated Hospital of the Air Force Military Medical University, Shaanxi, China) due to a left pelvis tumor. type II+III pelvic resection was performed and a customized prosthesis fabricated by 3D printing technology was implanted to reconstruct the pelvis. Four screws were used to fix the prosthesis during surgery and these four screws were numbered as 1 to 4 inside out starting from the medial pelvis (Fig. 1a).

2.2 Three-dimensional (3D) modeling

The CT images were obtained with the permission from the ethics committee of the hospital and then they were imported into Mimics 16.0 (Materialise, Belgium) for reconstructing triangle-based surface model of the pelvis. The pelvic surface model was imported into Geomagic Studio 2012 (Geomagic, USA) to create a solid model of the pelvis. Afterwards, the solid model was imported into Solidworks 2013 (Dassault, USA) for error checking and assembling the screws. The customized prosthesis was designed by using the topology optimization method and the details of the designing were described in our previous research[25]. Besides, two spherical shells were added at the acetabulum to simulate the femoral head in Abaqus/CAE (SIMULIA, USA) software. Finally, the 3D model of the RP was constructed (Fig. 1a). The natural pelvic model of the patient was obtained through the mirror image of the right ilium (Fig. 1b).

2.3 FE modeling

The material properties of the bones were determined according to the relationship between Hounsfield Units (HU) and bone density (ρ), as well as the relationship between bone density and Young's modulus (E) reported by Leung *et al*.[26]. The relations are as follows:

$$\rho = 0.00069141 \times \mathrm{HU} + 1.026716, \quad (1)$$

$$E = 2017.3\rho^{2.46}. \quad (2)$$

The material properties for the solid part of the prosthesis and the screws were defined as titanium alloy.

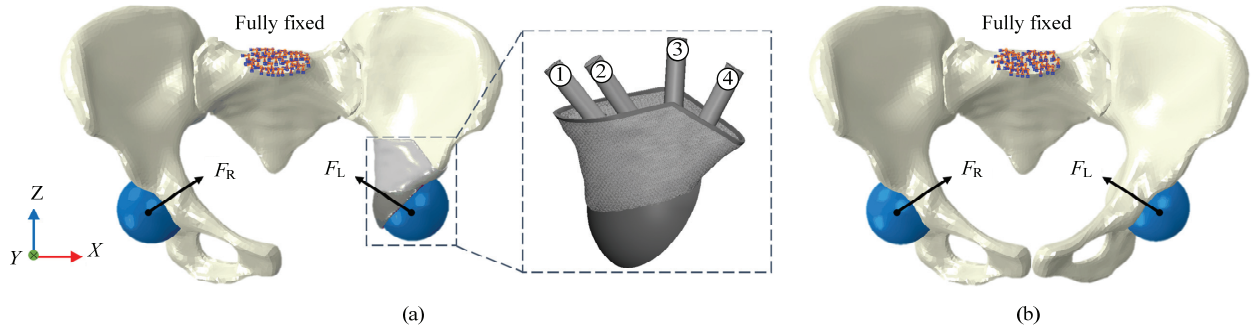

Fig. 1 Loading and boundary conditions for (a) RP and (b) NP. F_R and F_L refer to right and left hip Contact Force (CF) respectively.

The effective Young's modulus of the porous part of the prosthesis was 0.8 GPa, which was obtained by the experiment. All the material properties are shown in Table 1.

Tie constraints were used between the sacrum and ilia to simulate the sacroiliac joint[8]. The interface between bone and screws were also tied together to simulate the screw-thread fit[27]. Friction was set for the contact points between the prosthesis and bone as well as the interface between prosthesis and screws with a friction coefficient of 0.1[28]. Spring elements were used to simulate the pelvic ligaments according to the research of Hao *et al*.[21]. The parameters of these spring elements are shown in Table 2. Moreover, only the sacroiliac ligaments were included into the left side of RP due to the large resection.

The superior surfaces of S1 vertebra of NP and RP were fully constrained[14] and component forces presented in Fig. 2[29,30] were applied to the center of the rigid spherical shells along the *X*, *Y* and *Z* coordinate axes (Fig. 1) for simulating the routine activities of the pelvis. The hip contact forces were derived from the HIP 98 database.

For the meshed 3D models, four-node linear tetrahedron element (C3D4) was used for the bones and prosthesis, and 8-node linear element incompatible modes (C3D8I) was used for the screws. Moreover, 4-node 3-D bilinear rigid quadrilateral (R3D4) was used for the spherical shells. Mesh sensitivity analysis was conducted to eliminate the effect of meshing size. The optimal mesh size of 2 mm for bones and 1 mm for prosthesis as well as the screws were found to be sufficiently accurate (relative error of von Mises stress was less than 5%). The total number of elements for NP and RP is 118496 and 300772, respectively.

Table 1 Material properties used in present study

Component	Material	Young's modulus (GPa)	Poisson's ratio
Left ilium	Bone	2.22 – 9.68	0.3
Sacrum	Bone	1.99 – 9.25	0.3
Right ilium	Bone	2.04 – 9.80	0.3
Implant (solid)	Titanium alloy	110	0.3
Implant (porous)	Titanium alloy	0.8	0.3
Screws	Titanium alloy	110	0.3

Table 2 Parameters of the spring element

Ligament	Stiffness ($N \cdot mm^{-1}$)	Number of springs
Sacroiliac	5000	90
Sacrotuberous	1500	30
Sacrospinous	1500	12
Iliolumbar	1000	10
Arcuate pubic	500	15
Superior pubic	500	10

3 Results and discussion

3.1 Results

The maximum von Mises stresses of NP and RP models for the bone, screws as well as the implant during routine activities were predicted from the FE models and summarized in Fig. 3. Unlike the other gaits, the two-leg stance and one-leg stance are in static status. Therefore, other than a stress curve, only the maximum von Mises stresses are provided for these two gaits (Fig. 3a). The maximum stresses for two-leg stance and one-leg stance of NP are 11.9 MPa and 32.6 MPa. The maximum stresses of 10.1 MPa, 16.5MPa and 38.2 MPa were observed on the bone, screws and implant of the reconstructed pelvic model for two-leg stance. For one-leg stance, the maximum stresses of 38.4 MPa, 31.5 MPa and 68.4 MPa were observed on the bone, screws and implant of the reconstructed pelvic model, respectively. For the other seven gaits, the magnitude of the maximum stresses of NP and components of RP during the gait cycle are shown in Figs. 3b–3h.

The stress distribution of the NP for routine activities when maximum stress occurred is showed in Fig. 4. The stress is mainly concentrated around the upper part of the sacrum and the sacroiliac joint for the normal pelvic model under all the activities. Among all the activities, the minimum and maximum von Mises stresses of 11.9 MPa and 73.8 MPa were observed during two-leg stance and stair ascent, respectively. The maximum stress was observed around the superior surface of S1 vertebra for all the activities. Stress distribution of the pelvis was similar for sitting down and standing up. However, the maximum von Mises stress in the pelvis during standing up is 57.3 MPa, bigger than the peak stress value of 45.8 MPa during sitting down. Moreover, the stress distribution of the pelvis is similar for stair descent and stair ascent, however, the maximum von Mises stress during stair ascent is higher than that of stair descent.

F (Body weight, %)		F_x	F_y	F_z
Two-leg stance	L	−30.0	1.60	72.0
	R	30.0	1.60	72.0
One-leg stance	L	−23.2	0.43	202.1
	R	13.8	−8.70	24.2

(a)

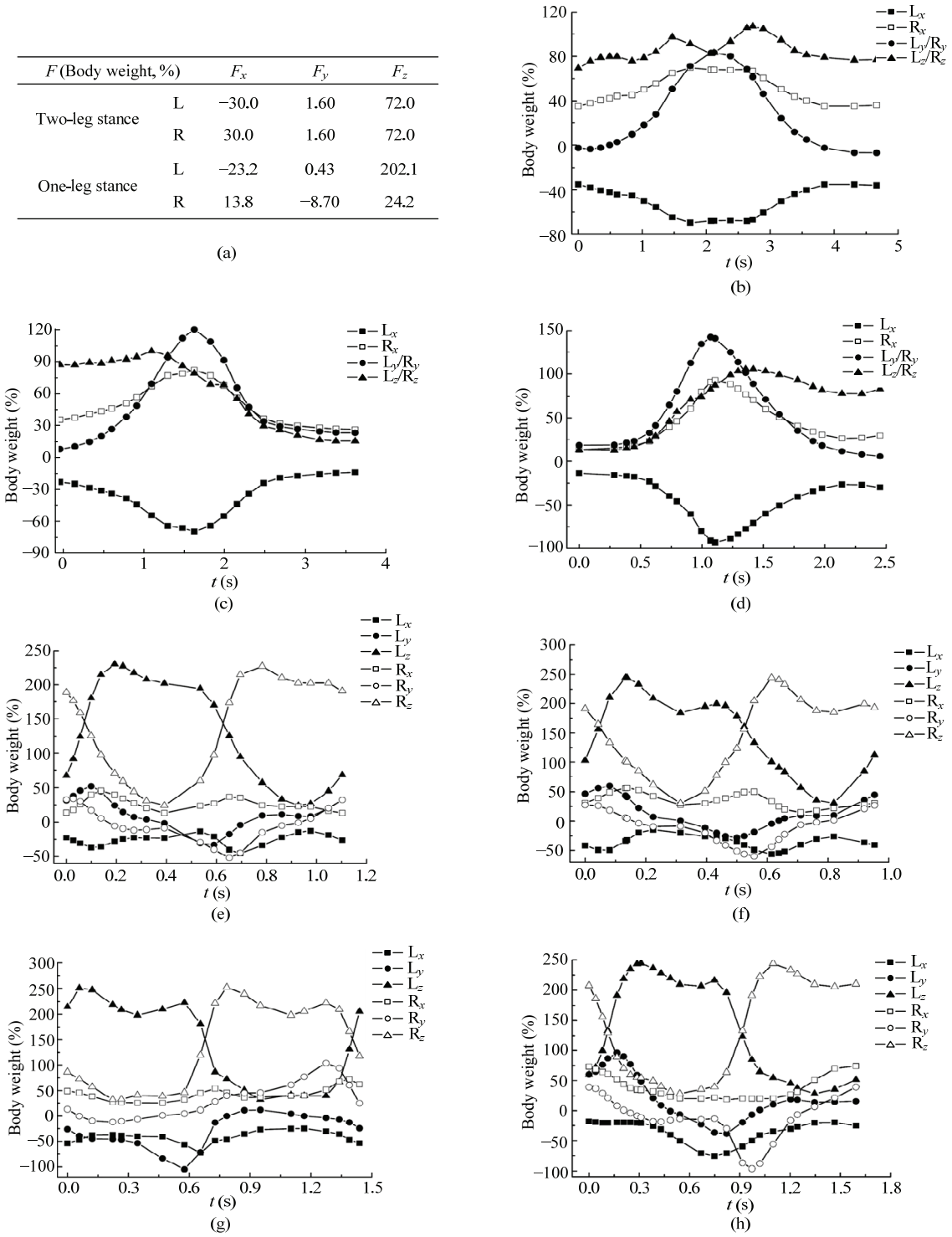

Fig. 2 Hip contact forces for (a) two-leg and one-leg stance, (b) knee bending, (c) sitting down, (d) standing up, (e) normal walking, (f) fast walking, (g) stair descent, (h) stair ascent. *t* refers to time. 'L' and 'R' refer to the left and right legs respectively. *x*, *y* and *z* subscripts refer to the *X*, *Y* and *Z* coordinate axes respectively (Fig. 1).

For the RP model, the stress distribution of the bone and prosthesis under routine activities is presented in Fig. 5 and Fig. 6, respectively. For the remaining part of the RP, the stress distribution is similar to that of the NP. The maximum von Mises stress of 67.9 MPa was observed during standing up for the bone. For the prosthesis,

Maximum von Mises stress (MPa)	NP	RP		
	Bone	Bone	Screws	Implant
Two-leg stance	11.9	10.1	16.5	38.2
One-leg stance	32.6	38.4	31.5	68.4

(a)

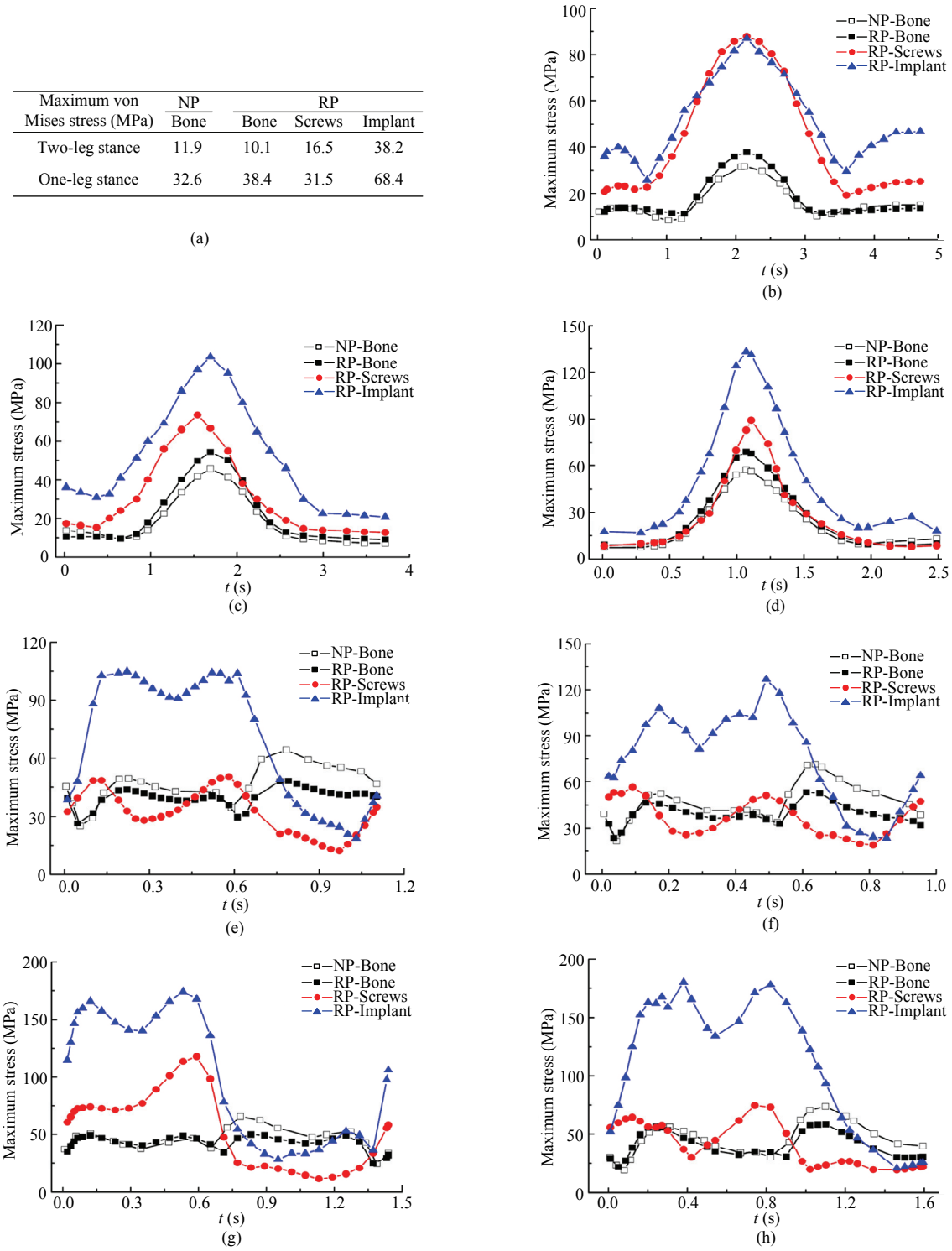

Fig. 3 Maximum von Mises stress of the NP and the components of the RP for (a) two-leg and one-leg stance, (b) knee bending, (c) sitting down, (d) standing up, (e) normal walking, (f) fast walking, (g) stair descent and (h) stair ascent. t refers to time.

the stress was concentrated around the interface of the bone and prosthesis as well as the junction of the solid part and porous part. The maximum von Mises stress is 180.2 MPa for the prosthesis during the stair ascent. As for the screws, the predicted stresses were mainly concentrated on screws 1 and 2 who were close to the medical

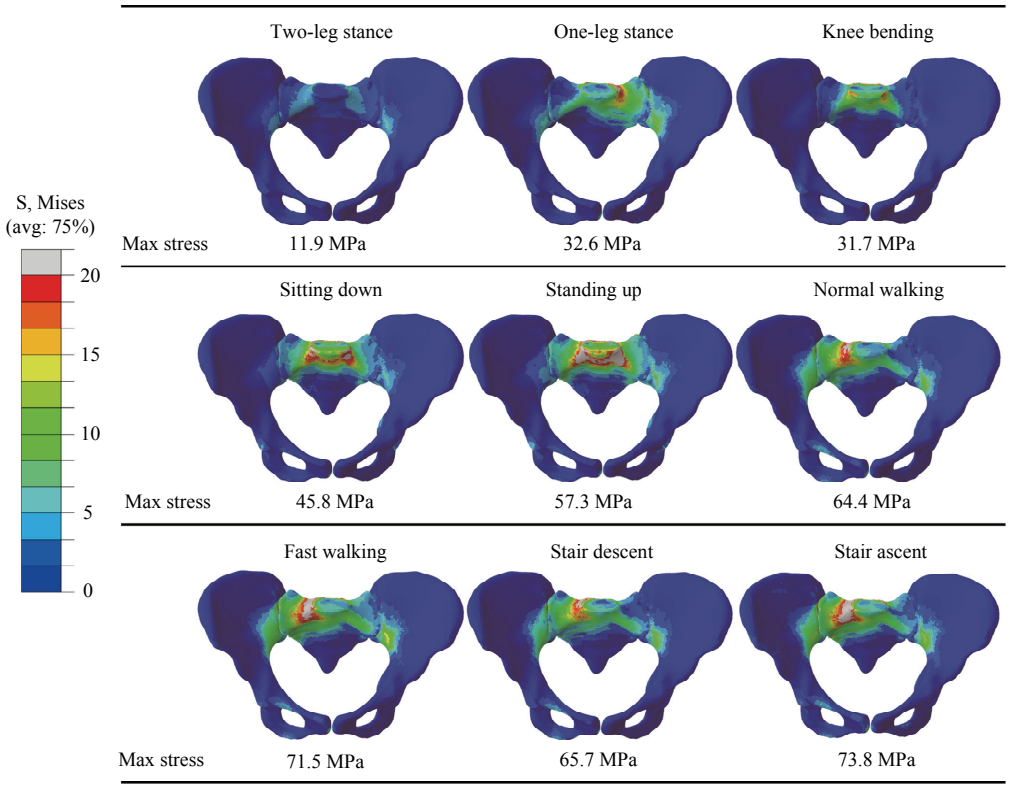

Fig. 4 Von Mises stress distribution of NP during routine activities.

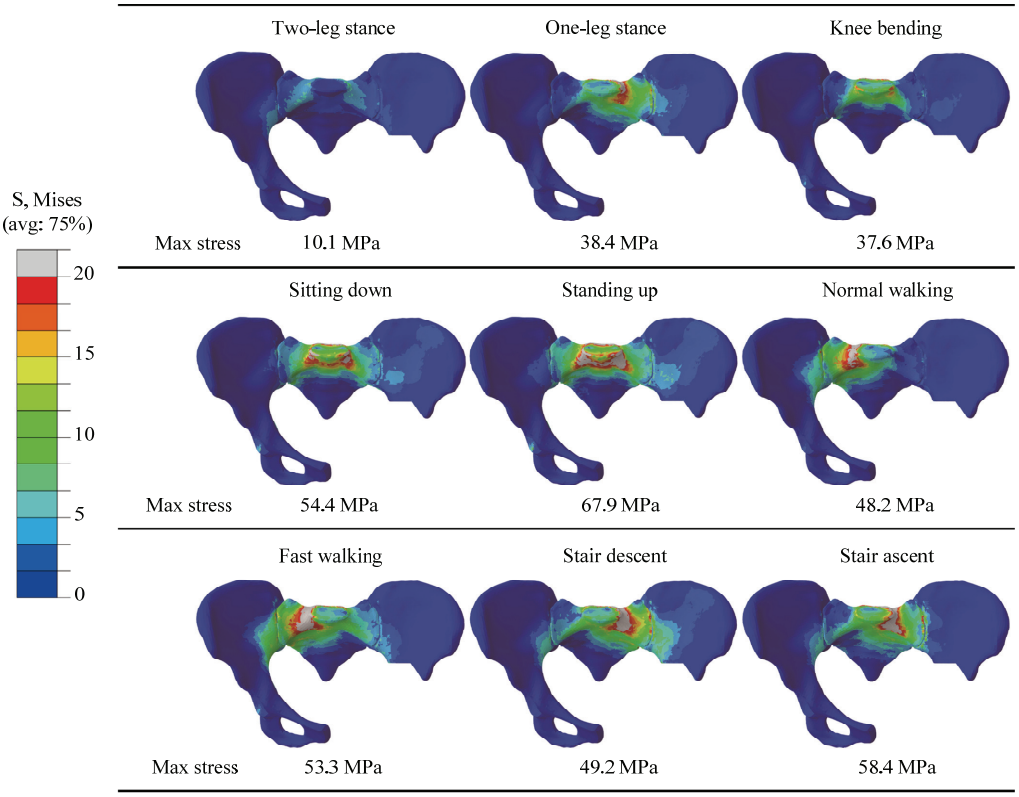

Fig. 5 Von Mises stress distribution of bone in RP during routine activities.

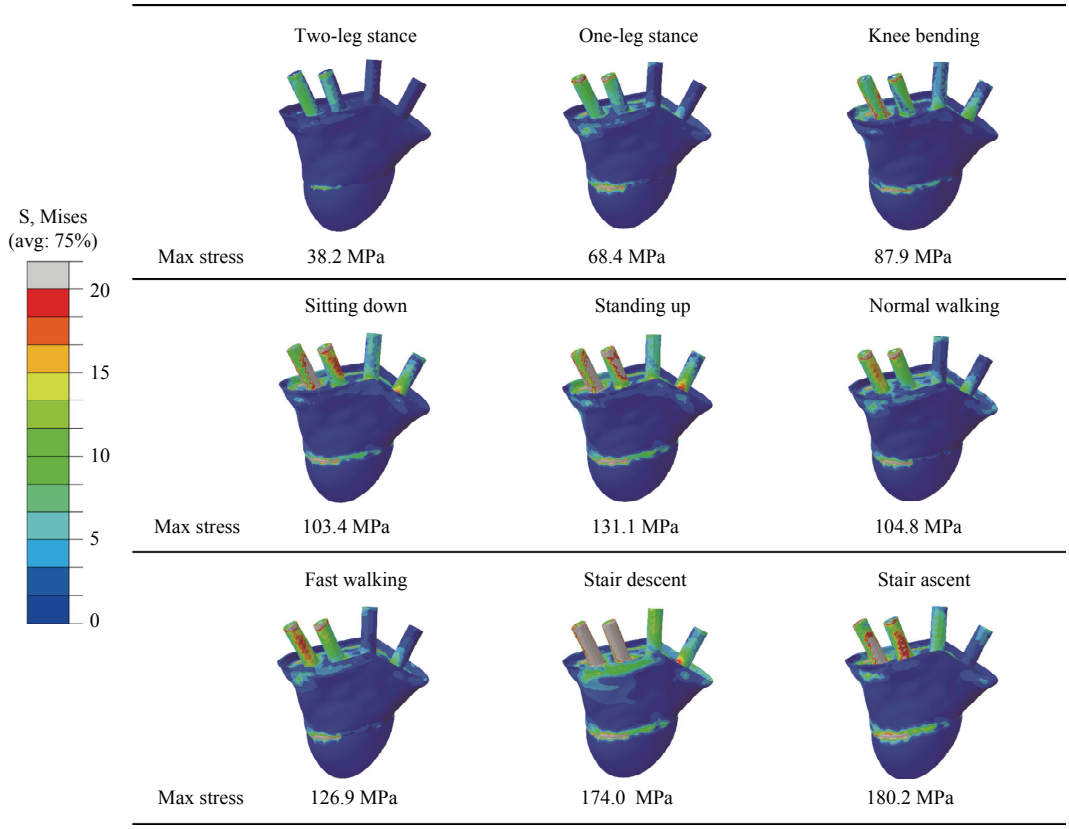

Fig. 6 Von Mises stress distribution of implant and screws in RP during routine activities.

side of the pelvis, and the maximum von Mises stress of 117.9 MPa was observed at the tip of screw 2 during stair descent. All the magnitude of maximum stresses for NP and components of RP under routine activities are summarized in Fig. 7.

Finally, the prosthesis was fabricated using Electron Beam Melting (EBM) technology, with 20 μm – 53 μm diameter of Ti-6Al-4V powder. The processing parameters include: the layer thickness of 50 μm, scanning distance of 0.08 mm – 0.1mm, scanning speed of 1000 $mm \cdot s^{-1}$ – 1300 $mm \cdot s^{-1}$. The prosthesis was successfully implanted into the patient at Xijing Hospital (Fig. 8). The patient was kept in bed allowing for the pelvic-surrounding tissue to healing for two weeks postoperatively. Thereafter, she could walk with the assistants of canes or walker, and the weight was mostly borne *via* the contralateral limb and toe-touching was allowed for the involved limb. After six weeks, the patient has obtained full ambulatory status with gait aids. Unfortunately, the patient died of metastasis three months postoperatively, with no sign of implant loosening or infection.

3.2 Discussion

Based on a clinical case of pelvic II+III reconstruction, a customized prosthesis was designed and a functional evaluation methodology was established for prostheses under different daily activities in this study. The FE models of NP and RP were built and the biomechanical performance of the normal and reconstructed pelvic model was investigated for multi-activities including standing, knee bending, sitting down, standing up, walking, stair descent and stair ascent. Moreover, the strength and stability of the prosthesis were evaluated under these activities.

For the natural pelvic model, the stress is mainly distributed around the upper part of the sacrum and the sacroiliac joint (Fig. 4). Stair ascent is the most dangerous gait among all the routine activities for NP. The maximum von Mises stress during stair ascent is 73.8 MPa, which is close to the strength of the cortical bone (80 MPa – 150 MPa)[31]. Advices for designing

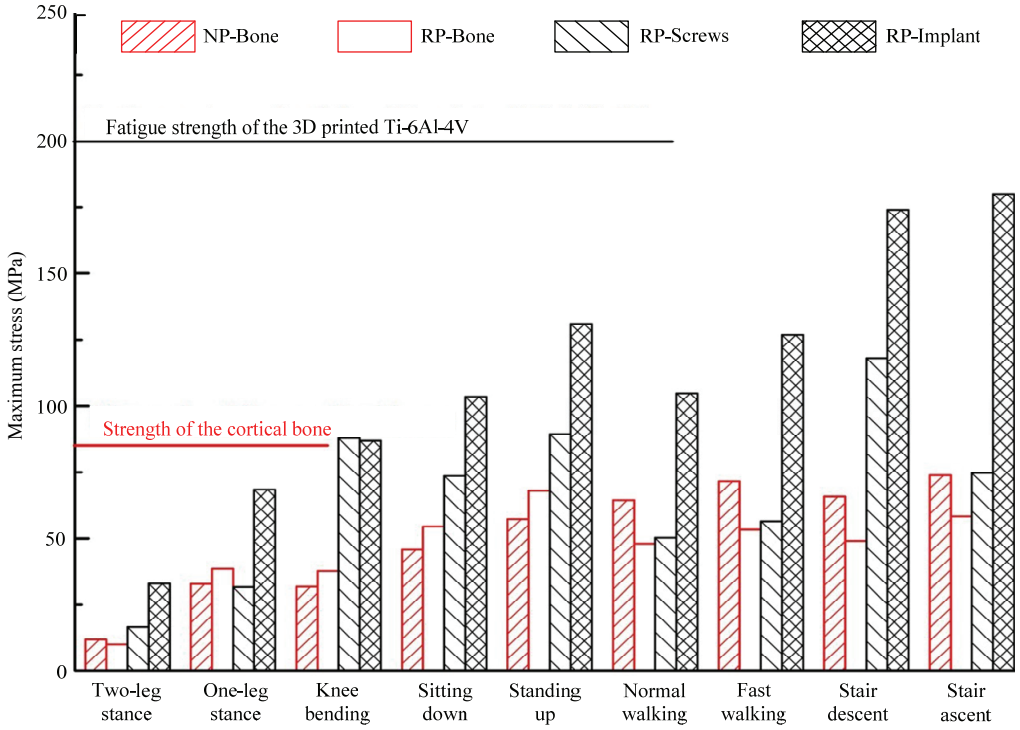

Fig. 7 Maximum von Mises stress of NP and components of RP during routine activities. The strength of cortical bone[31] and the fatigue strength of the typical 3D printed Ti-6Al-4V[32] are provided as references.

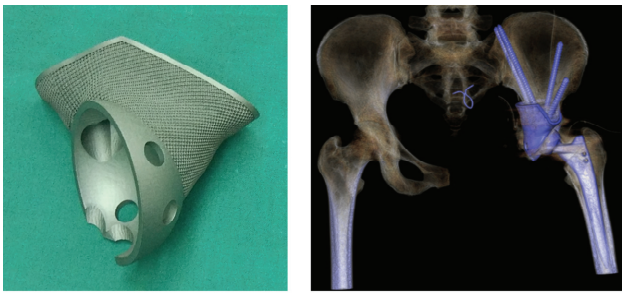

(a) (b)

Fig. 8 (a) 3D-printed prosthesis and (b) X-ray image of the reconstructed pelvis after clinical implantation (provided by Xijing Hospital).

prostheses of different types can be provided from the stress distribution. As the stress is mainly transferred through the sacroiliac joint, it should be very careful when design the fixation part of the prostheses to connect the joint for type I reconstruction. Moreover, like the prosthesis presented in this article, the sitting bone is not reconstructed for type II+III because the sitting bone bears minimum stress and smaller prosthesis could reduce the risk of infection.

For the residual bone of the reconstructed pelvic model, the stress distribution is very similar to that of the NP bone, *i.e.*, mainly concentrating at the upper part of the sacrum and the sacroiliac joint. Meanwhile, according to the results presented in Fig. 3, the magnitude and variation of the maximum von Mises stress for the NP and the remaining bone of RP are similar (below 25%) to each other for all the routine activities. However, the maximum von Mises stress of the RP remaining bone is 67.9 MPa during standing up, rather than during stair ascent. This might be due to the large displacement that the pelvis moved, as well as large range of motion at the hip joint, which made the standing up the most dangerous instance for the pelvic replacement patient.

The stress on the implant is mainly distributed around the interface between the residual bone and the implant as well as the junction of the solid and porous part. The maximum von Mises stress of the implant is observed during stair ascent and the magnitude is 180.2 MPa, which is slightly below the fatigue strength of the 3D printed Ti-6Al-4V (200 MPa – 500 MPa)[32] and far below the yield strength of Ti-6Al-4V (789 MPa – 1013 MPa)[33]. Even through the maximum von Mises stress for the porous part of the implant has exceeded the fatigue strength (13.6 MPa)[34] of the porous structure,

the mechanical performance, especially for the fatigue strength of the porous structure will be dramatically improved with the bone in growth[35]. Meanwhile, as the results presented in Fig. 6, the stress on the porous part is mainly concentrated at the junction with the solid part due to the high stiffness mismatch between the solid and porous part of the implant[36]. Graded porous structure can provide a gradual change of the material property from the solid to porous part, which might reduce such a stress concentration[37,38].

Four screws were used to connect the implant and the left ilium during the surgery. The maximum von Mises stress of the screws was observed during stair descent and the magnitude was 117.9 MPa, which is much lower than the fatigue strength of the traditional methods made Ti-6Al-4V (310 MPa – 610 MPa)[39]. However, as the results showed in Fig. 6, the stress is mainly concentrated on the two screws closed to the inside pelvis (screws 1 and 2) compared to the other two screws (screws 3 and 4). For example, the maximum von Mises stress is 92.3 MPa, 117.9 MPa, 46.6 MPa and 34.9 MPa for the screws 1 to 4 during stairs descent, respectively. This means four screws might be not necessary for such design. It is not always the case that more screws can be better for fixing the prosthesis since some of the screws might bear minimum load[20]. Additionally, more screws are associated with more traumas and greater risk of infection. Thus, it is important to optimize the number of screws whilst ensuring the stability of the prosthesis[20].

According to the hip joint contact forces summarized in Fig. 2, the peak value of the hip joint contact force is varying from 0.7- times to 2.6-times of the body weight under routine activities. The peak value of contact forces are more than 2.5 times of the body weight for fast walking, stair ascent and stair descent gait, which indicated these gaits are the dangerous activities for the reconstructed pelvis. However, it is not always that bigger joint contact force means more risk for the pelvis. It is also influenced by many factors such as the individual anatomy and properties of the pelvis, the resection type, the prosthesis designing, the fixation type and so on. For example, for the case reported in this research, stair ascent is the most dangerous gait for the NP, however, for the residual bone, implant and the screws of the RP, the maximum von Mises stress was observed during standing up, stair ascent and stair descent, respectively. Therefore, it is important to understand the biomechanical performance of the NP and to evaluate the strength as well as the stability of the prosthesis especially for the customized prosthesis in all the routine activities.

4 Conclusion

In this study, a customized prosthesis was designed for the pelvic type II+III reconstruction. For the functional evaluation of the designed prosthesis, FE model of both the normal and reconstructed pelvis were built, and the biomechanics of the reconstructed pelvis were studied under multi-daily activities. For the normal pelvic model, the stress mainly concentrates around the upper part of the sacrum and the sacroiliac joint during all the activities and the maximum stress occurred during stair ascent. As for the reconstructed pelvis, the stress distribution and tendency of the maximum stress variation of the bone part during all the activities are very similar to those of the normal pelvic model, which indicates that the load transferring function of the RP could be restored by the customized prosthesis. Moreover, the maximum von Mises stress of the customized prosthesis and the screws are below the fatigue strength of the 3D printed Ti-6Al-4V, which indicates the customized prosthesis would have a reliable mechanical performance after implantation. It is critically necessary to evaluate the mechanical performance of the customized prosthesis under various daily activities to identify the worst severe conditions so that advices could be provided to avoid dangerous activities, and strength/stability could be checked before clinical applications.

Acknowledgment

The work was supported by the Program of the National Key R&D Program of China (2018YFC11067000), National Key R&D Program of China (2018YFB1107000), Key R&D Program of Guangdong Province (2018B090906001), the Key Program of International Cooperation in Shaanxi Province (2017KW-ZD-02), the Fundamental Research Funds for the Central Universities and the Youth Innovation Team of Shaanxi Universities, Project of Scientific Research

of Shaanxi (2016SF-136).

References

[1] Phillips A T M, Pankaj P, Howie C R, Usmani A S, Simpson A H R W. Finite element modelling of the pelvis: Inclusion of muscular and ligamentous boundary conditions. *Medical Engineering & Physics*, 2007, **29**, 739–748.

[2] Jia Y W, Cheng L M, Yu G R, Du C F, Yang Z Y, Yu Y, Ding Z Q. A finite element analysis of the pelvic reconstruction using fibular transplantation fixed with four different rod-screw systems after type I resection. *Chinese Medical Journal*, 2008, **121**, 321–326.

[3] Liu D X, Hua Z K, Yan X Y,Jin Z M. Design and biomechanical study of a novel adjustable hemipelvic prosthesis. *Medical Engineering & Physics*, 2016, **38**, 1416–1425.

[4] Wang B, Sun P D, Xie X B, Wu W D, Tu J, Ouyang G J, Shen J N. A novel combined hemipelvic endoprosthesis for peri-acetabular tumours involving sacroiliac joint: A finite element study. *International Orthopaedics*, 2015, **39**, 2253–2259.

[5] Bus M P A, Campanacci D A, Albergo J I, Leithner A, Van de Sande M A J, Michiel A J, Gaston C L, Caff G, Mettelsiefen J, Capanna R,Tunn P U. Conventional primary central chondrosarcoma of the pelvis. *The Journal of Bone and Joint Surgery*, 2018, **100**, 316–325.

[6] Noakes K F, Bissett I P, Pullan A J, Cheng L K. Anatomically realistic three-dimensional meshes of the pelvic floor & anal canal for finite element analysis. *Annals of Biomedical Engineering*, 2008, **36**, 1060–1071.

[7] Ji T, Guo W, Tang X D, Yang Y. Reconstruction of type II+III pelvic resection with a modular hemipelvic endoprosthesis: A finite element analysis study. *Orthopaedic Surgery*, 2010, **2**, 272–277.

[8] Iqbal T, Shi L, Wang L, Liu Y X, Li D C, Qin M, Jin Z M. Development of finite element model for customized prostheses design for patient with pelvic bone tumor. *Journal of Engineering in Medicine*, 2017, **231**, 525–533.

[9] Zhou Y, Min L, Liu Y, Shi R, Zhang W L, Zhang H, Duan H, Tu C Q. Finite element analysis of the pelvis after modular hemipelvic endoprosthesis reconstruction. *International Orthopaedics*, 2013, **37**, 653–658.

[10] Kitagawa Y, Ek E T, Choong P F M. Pelvic reconstruction using saddle prosthesis following limb salvage operation for periacetabular tumour. *Journal of Orthopaedic Surgery*, 2006, **14**, 155–162.

[11] Donati D, D'Apote G, Cevolani L, Benedetti M G. Clinical and functional outcomes of the saddle prosthesis. *Journal of Orthopaedics & Traumatology*, 2012, **13**, 79–88.

[12] Aljassir F, Beadel G P, Turcotte R E, Griffin A M, Bell R S, Wunder J S, Isler M H. Outcome after pelvic sarcoma resection reconstructed with saddle prosthesis. *Clinical Orthopaedics & Related Research*, 2005, **438**, 36–41.

[13] Issa S P, Biau D, Babinet A, Dumaine V, Hanneur M L,Anract P. Pelvic reconstructions following peri-acetabular bone tumour resections using a cementless ice-cream cone prosthesis with dual mobility cup. *International Orthopaedics*, 2018, **42**, 1987–1997.

[14] Liu D X, Hua Z K, Yan X Y, Jin Z M. Biomechanical analysis of a novel hemipelvic endoprosthesis during ascending and descending stairs. *Journal of Engineering in Medicine*, 2016, **230**, 962–975.

[15] Zhao X, Xiao J L, Sun Y, Zhu Z, Xu M, Wang X N, Lin F F, Wang Y B, Wang J C. Novel 3D printed modular hemipelvic prosthesis for successful hemipelvic arthroplasty: A case study. *Journal of Bionic Engineering*, 2018, **15**, 1067–1074.

[16] Wang B, Xie X B, Yin J Q, Zou C Y, Wang J, Huang G, Wang Y Q, Shen J N. Reconstruction with modular hemipelvic endoprosthesis after pelvic tumor resection: A report of 50 consecutive cases. *PLoS One*, 2015, **10**, e0127263

[17] Ying T, Ma R Y, Ming Y, Wang D M, Wang C T. Rapid prototyping fabrication and finite element evaluation of the three-dimensional medical pelvic model. *International Journal of Advanced Manufacturing Technology*, 2006, **28**, 302–306.

[18] Guo W, Li D S, Tang X D, Yang Y, Ji T. Reconstruction with modular hemipelvic prostheses for periacetabular tumor. *Clinical Orthopaedics & Related Research*, 2007, **461**, 180–188

[19] García J M, Doblaré M, Seral B, Seral F, Palanca D, Gracia L. Three-dimensional finite element analysis of several internal and external pelvis fixations. *Journal of Biomechanical Engineering*, 2000, **122**, 516–522

[20] Dong E C, Ling W, Iqbal T, Li D C, Liu Y X, He J K, Zhao B H, Li Y. Finite element analysis of the pelvis after customized prosthesis reconstruction. *Journal of Bionic Engineering*, 2018, **15**, 443–451

[21] Hao Z X, Wan C, Gao X F, Ji T. The effect of boundary condition on the biomechanics of a human pelvic joint under an axial compressive load: A three-dimensional finite element model. *Journal of Biomechanical Engineering*, 2011, **8**, 965–979

[22] Fan Y P, Lei J Y, Zhu F, Li Z Q, Chen W Y, Liu X M. Biomechanical analysis of the fixation system for T-shaped acetabular fracture. *Computational & Mathematical Me-*

thods in Medicine, 2015, **2015**, 370631.

[23] Zhou Y, Min L, Liu Y, Shi R, Zhang W L, Zhang H, Duan H, Tu C Q. Finite element analysis of the pelvis after modular hemipelvic endoprosthesis reconstruction. *International Orthopaedics*, 2013, **37**, 653–658

[24] Volinski B, Kalra A,Yang K. Evaluation of full pelvic ring stresses using a bilateral static gait-phase finite element modeling method. *Journal of the Mechanical Behavior of Biomedical Materials*, 2017, **78**, 175–187.

[25] Iqbal T, Wang L, Li D C, Dong E C, Fan H B, Fu J, Hu C. A general multi-objective topology optimization methodology developed for customized design of pelvic prostheses. *Medical Engineering and Physics*, 2019, **69**, 8–16.

[26] Leung A S O, Gordon L M, Skrinskas T, Szwedowski T, Whyne C M. Effects of bone density alterations on strain patterns in the pelvis: Application of a finite element model. *Proceedings of the Institution of Mechanical Engineers*, *Part H*: *Journal of Engineering in Medicine*. 2009, **223**, 965–979

[27] Hao Z X, Wan C, Gao X F, Ji T,Wang H S. The effect of screw fixation type on a modular hemi-pelvic prosthesis: A 3-D finite element model. *Disability & Rehabilitation Assistive Technology*, 2013, **8**, 125–128

[28] Andersen R C, O'Toole R V, Nascone J W, Sciadini M F, Frisch H M, Turen C W. Modified stoppa approach for acetabular fractures with anterior and posterior column displacement: Quantification of radiographic reduction and analysis of interobserver variability. *Journal of Orthopaedic Trauma*, 2010, **24**, 271–278

[29] Bergmann G, Graichen F, Rohlmann A. Hip joint loading during walking and running, measured in two patients. *Journal of Biomechanics*, 1993, **26**, 969–990

[30] Mann R W. Comment on: Hip contact forces and gait patterns from routine activities. *Journal of Biomechanics*, 2002, **35**, 719–720

[31] Reilly D T, Burstein A H. The Mechanical properties of cortical bone. *Journal of Bone and Joint Surgery*, 1974, **56**, 1001–1022

[32] Greitemeier D, Palm F, Syassen F, Melz T. Fatigue performance of additive manufactured TiAl6V4 using electron and laser beam melting. *International Journal of Fatigue*, 2017, **94**, 211–217

[33] Hosseini S, Hudak R, Penhaker M, Majernik J. Fatigue of Ti-6Al-4V. *Biomedical Engineering Technical Applications in Medicine*, 2012, **17**, 75–92

[34] Zhao S, Li S J, Hou W T, Hao Y L, Yang R, Misra R D K. The influence of cell morphology on the compressive fatigue behavior of Ti-6Al-4V meshes fabricated by electron beam melting. *Journal of the Mechanical Behavior of Biomedical Materials*, 2016, **59**, 251–264

[35] Hedayati R, Janbaz S, Sadighi M, Mohammadi-Aghdam M, Zadpoor A A. How does tissue regeneration influence the mechanical behavior of additively manufactured porous biomaterials? *Journal of the Mechanical Behavior of Biomedical Materials*, 2017, **65**, 831–841

[36] Dumas M, Terriault P, Brailovski V. Modelling and characterization of a porosity graded lattice structure for additively manufactured biomaterials. *Materials & Design*, 2017, **121**, 383–392

[37] Simoneau C, Brailovski V, Terriault P. Design, manufacture and tensile properties of stochastic porous metallic structures. *Mechanics of Materials*, 2016, **94**, 26–37

[38] Wang L, Kang J F, Sun C N, Li D C, Cao Y, Jin Z M. Mapping porous microstructures to yield desired mechanical properties for application in 3D printed bone scaffolds and orthopaedic implants. *Materials & Design*, 2017, **133**, 62–68

[39] Long M, Rack H J. Titanium alloys in total joint replacement—A materials science perspective. *Biomaterials*, 1998, **19**, 1621–1639.